

## Oscillations of Chiral Preference in Proline Clusters

Alison E. Holliday,<sup>†</sup> Natalya Atlasevich,<sup>‡</sup> Sunnie Myung,<sup>§</sup> Manolo D. Plasencia,<sup>||</sup> Stephen J. Valentine,<sup>‡</sup> and David E. Clemmer<sup>\*,‡</sup>

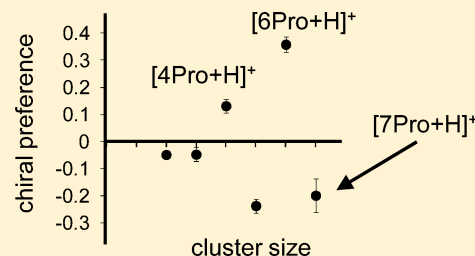
<sup>†</sup>Department of Chemistry and Biochemistry, Swarthmore College, Swarthmore, Pennsylvania 19081, United States

<sup>‡</sup>Department of Chemistry, Indiana University, Bloomington, Indiana 47405, United States

<sup>§</sup>Merck Research Laboratories, Union, New Jersey 07083, United States

<sup>||</sup>Department of Chemistry, Washington University, St. Louis, Missouri 63110, United States

**ABSTRACT:** Ion mobility/mass spectrometry techniques are used to study the chiral preferences of small proline clusters (containing 2 to 23 proline monomers) produced by electrospray ionization. By varying the composition of the electrospray solution from enantiomerically pure (100% L or 100% D) to racemic (50:50 L:D), it is possible to delineate which cluster sizes prefer homochiral (resolved) or heterochiral (antiresolved) compositions. The results show a remarkable oscillation in chiral preference. Singly protonated clusters,  $[x\text{Pro}+\text{H}]^+$  (where  $x$  corresponds to the number of prolines), favor homochiral assemblies (for  $x = 4, 6, 11$  and  $12$ ); heterochiral structures are preferred (although the preferences are not as strong) for  $x = 5$  and  $7$ . Larger, doubly protonated clusters  $[x\text{Pro}+2\text{H}]^{2+}$  favor homochiral assemblies for  $x = 18, 19,$  and  $23$  and heterochiral structures for  $x = 14, 16, 17, 20, 21,$  and  $22$ . Some of the variations that are observed can be rationalized through simple structures that would lead to especially stable geometries. It is suggested that some antiresolved clusters, such as  $[22\text{Pro}+2\text{H}]^{2+}$ , may be comprised of resolved D- and L-proline domains.



### INTRODUCTION

Although chiral resolution of racemic solutions to form D- and L-crystals is a rare phenomenon,<sup>1</sup> recent studies indicate that some small clusters of amino acids exhibit strong chiral preferences.<sup>2–10</sup> This has been highlighted in studies of serine.<sup>2–4,11–17</sup> Solvent evaporation from racemic serine solutions leads to the formation of racemic crystals; however, when solvent is removed during the process of electrospraying solutions into the gas phase, small clusters of D- or L-octamers spontaneously resolve. It has been proposed that this is because  $[8\text{Ser}+\text{H}]^+$  assembles into an especially stable cubic geometry that is favored as one of the enantiomers becomes enriched.<sup>2,4,18,19</sup> Recent reports involving proline indicate that  $[12\text{Pro}+\text{H}]^+$  also shows a propensity to resolve. Theory suggests that this cluster assembles into unusually stable, icosahedral-like geometries, in which the single proton is trapped inside a hollow cluster interior.<sup>20</sup>

Despite the large differences in the proposed geometries for  $[8\text{Ser}+\text{H}]^+$  and  $[12\text{Pro}+\text{H}]^+$ , it is apparently important that each proposed structure is closed. In systems that assemble (such as clusters), closed structures are interesting because often inclusion of another monomer leads to a geometry in which one unit of the cluster is weakly bound; additionally, removal of a monomer from a closed geometry creates a defect that is destabilizing. Thus, stable structures become favored in abundance. This type of behavior is well-known in the field of atomic clusters.<sup>21,22</sup> For clusters in which electrons are delocalized, electronic shell closings favor specific cluster sizes; moreover, these systems (as well as those that favor

covalent bonding interactions such as  $\text{C}_{60}$ )<sup>23</sup> often favor highly symmetric closed geometries. Molecular clusters also show this behavior; for example, the  $[21\text{H}_2\text{O}+\text{H}]^+$  cluster is believed to favor a structure in which 20 water molecules sit at the vertices of a dodecahedron that encapsulates a single  $\text{H}_3\text{O}^+$ .<sup>24</sup> Such water clathrate geometries have been proposed around charged residues in partially solvated proteins and peptides produced by electrospray.<sup>25–27</sup> Finally, we note that closed assemblies also persist to very large sizes; examples range from relatively small protein complexes to larger structures such as the protein capsids of viruses.<sup>28</sup>

In the present work, we examine how chirality influences cluster formation for relatively small clusters of D- and L-proline (containing from 2 to 23 proline monomer units). Our experimental findings indicate that this system displays a remarkable oscillation in chiral preference. Small, singly protonated clusters  $[x\text{Pro}+\text{H}]^+$  (where  $x$  corresponds to the number of prolines) are predominantly homochiral where  $x = 4, 6, 11,$  and  $12$ . The odd numbered sizes ( $x = 5$  and  $7$ ) are preferentially heterochiral. Larger doubly protonated  $[x\text{Pro}+2\text{H}]^{2+}$  ions favor homochiral compositions for  $x = 18, 19,$  and  $23$  and mixed L:D compositions for  $x = 14, 16, 17, 20, 21,$  and  $22$ . We propose that such oscillations may arise if mixed

**Special Issue:** Peter B. Armentrout Festschrift

**Received:** March 20, 2012

**Revised:** June 5, 2012

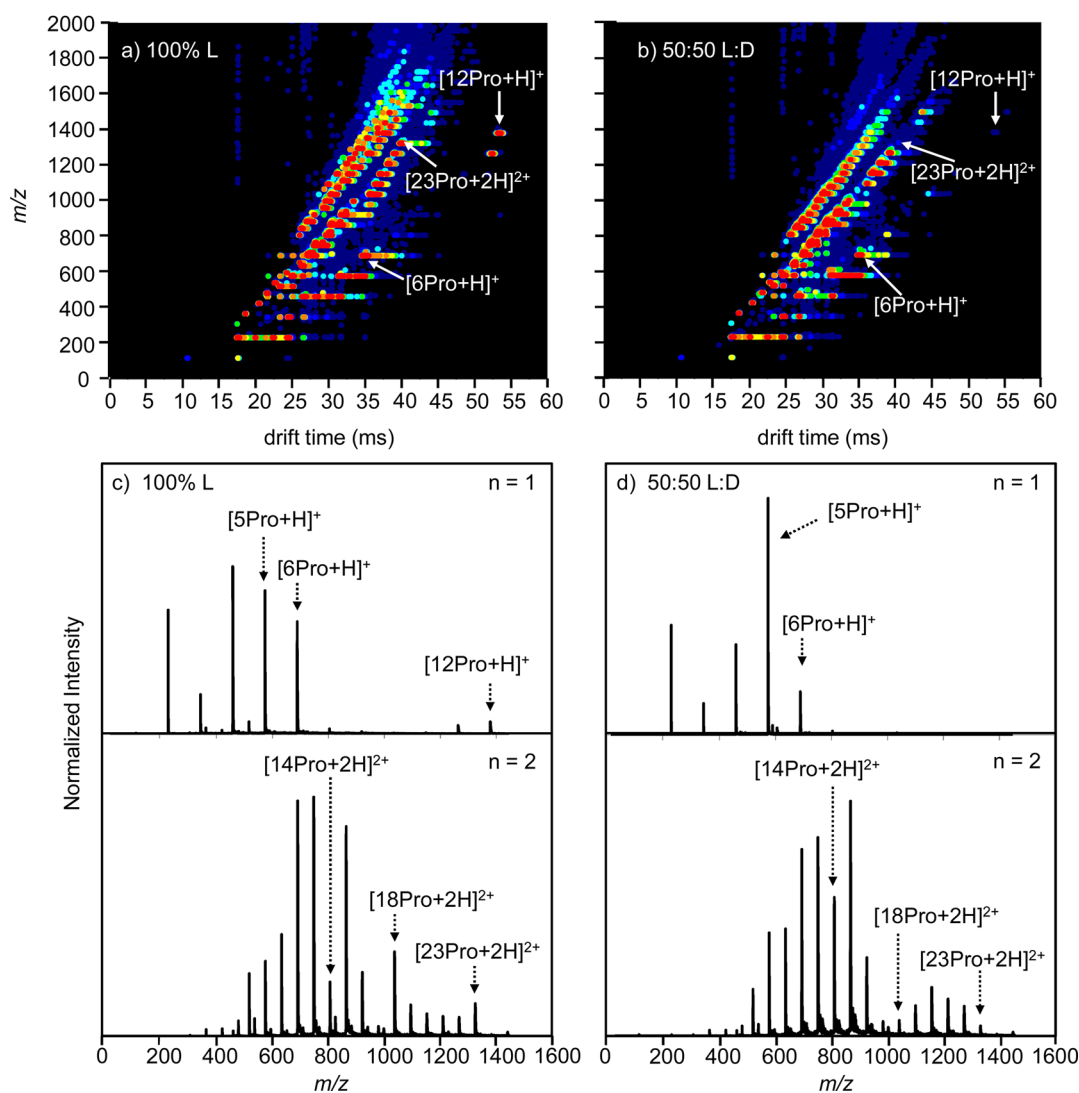


**Figure 1.** Two-dimensional plot of drift time (ms) versus  $m/z$  ratios for an electrosprayed 0.01 M solution of (a) enantiopure (100% L) and (b) racemic (50:50 L:D) proline. The mass spectra below were obtained by integrating across narrow regions of the (c) enantiopure and (d) racemic two-dimensional data sets for the  $n = 1$  (top) and 2 (bottom) charge state families. The intensity of different features is shown using a false color scheme in which the least intense features are represented in navy and the most intense features are represented in red.

clusters exist as preresolved assemblies, i.e., assemblies with D- and L- domains within the heterochiral complex.

## EXPERIMENTAL SECTION

**Overview.** Ion-mobility spectrometry (IMS) techniques have been described in detail previously.<sup>29–42</sup> Only a brief description of the experimental approach employed for cluster characterization is presented here. Proline cluster ions are generated by electrospray ionization (ESI) and are trapped in an hourglass ion funnel<sup>38</sup> inside a differentially pumped desolvation region. Mobility measurements are initiated by gating packets of ions (150  $\mu$ s in duration) from the funnel into a drift tube ( $\sim 289$  cm) that is filled with  $\sim 3.0$  Torr of 300K He buffer gas. Ions with different mobilities separate in the drift tube under the influence of a weak uniform electric field ( $\sim 10$  V $\cdot$ cm $^{-1}$ ). The high-resolution IMS-MS prototype instrument used in these experiments has been described previously.<sup>43,44</sup> Three ion funnels are placed strategically in the drift tube to concentrate diffuse ion clouds in order to improve the efficiency of ion transmission. Upon exiting the drift tube,

ions enter the source region of an orthogonal-extraction time-of-flight (TOF) mass spectrometer. Flight times in the mass spectrometer are much shorter than drift times through the IMS instrument, making it possible to record drift and flight times using a nested approach that has been described previously.<sup>35</sup>

Drift times are converted to collision cross sections using the expression:<sup>29</sup>

$$\Omega = \frac{(18\pi)^{1/2}}{16} \frac{ze}{(k_b T)^{1/2}} \left[ \frac{1}{m_i} + \frac{1}{m_b} \right]^{1/2} \frac{t_D E}{L} \frac{760}{P} \frac{T}{273.2 N} \quad (1)$$

In eq 1,  $ze$ ,  $k_b$ ,  $m_i$ , and  $m_b$  correspond to the ion's charge, Boltzmann's constant, the mass of the ion, and the mass of the buffer gas (He in this work), respectively. The variables  $E$  and  $L$  are the electric field and the drift length, respectively.  $P$  and  $T$  correspond to the buffer gas pressure and temperature, respectively.  $N$  is the neutral number density of the buffer gas at STP conditions.

**Sample Preparation.** L- and D-proline (Fluka, 99% purity), and deuterated L-proline ( $\text{HN}(\text{CD}_2)_3\text{CDCOOH}$ ) (Cambridge Isotope Laboratories, Inc.,  $\geq 98\%$  purity) were used without further purification. All solutions were prepared in 49:49:2 water:acetonitrile:acetic acid at a total concentration of 0.01 M. Solutions were electrosprayed with a flow rate of  $0.1 \mu\text{L}\cdot\text{min}^{-1}$  through a pulled fused silica capillary tip made in-house (100  $\mu\text{m}$  i.d., 360  $\mu\text{m}$  o.d., Polymicro). The solution in the capillary is biased  $\sim +2500$  V above the ESI desolvation region entrance aperture.

**Analysis of Chiral Preference.** Chiral preferences were determined by two methods: one involving the use of unlabeled mixtures,<sup>8</sup> and another involving the use of a mixture containing deuterated L-proline.<sup>3,11</sup> In the former (unlabeled) approach, seven solutions comprised of L:D compositions of 100:0, 80:20, 60:40, 50:50, 40:60, 20:80, and 0:100 were electrosprayed into an ion-mobility/mass spectrometry (IMS-MS) instrument. The ability to separate isobaric ions in an IMS-MS instrument allows for quantitative analysis of individual cluster sizes without complications resulting from isobaric interferences. Mass spectra of individual charge state families are obtained by integrating regions across the two-dimensional drift time ( $m/z$ ) data set, and intensity information about individual clusters are obtained from these spectra for chiral preference determination. The chiral preference of a cluster is determined by measuring its abundance relative to the total ion intensity as the composition of the solution is varied from enantiomerically pure (100% L or 100% D) to racemic (50:50 L:D) amino acid.

The labeled approach allows the propensities to form mixed or resolved clusters to be measured directly. In this case, the intensity information of specific cluster compositions is compared with values that are calculated for a statistical distribution to determine whether a preference exists. This method is complicated in that each cluster size splits into  $x + 1$  peaks (where  $x$  is the number of monomer units). Peaks associated with varying deuterated compositions for different cluster sizes overlap for large clusters. Therefore this approach is used here as a cross-check of chiral preferences determined for relatively small clusters.

## RESULTS AND DISCUSSION

**IMS-MS spectra.** Figure 1 shows typical two-dimensional nested ion mobility mass spectra<sup>35</sup> obtained by electrospraying 0.01 M solutions of enantiopure (100% L) and racemic (50:50 L:D) proline. Peaks fall into families according to their charge state and size, designated here by  $[x\text{Pro}+n\text{H}]^{n+}$ , where  $n$  corresponds to the charge state and  $x$  refers to the number of monomer units in the cluster, as noted above. Clusters corresponding to ions for which  $n = 1$  to 4 are the dominant features in these spectra. In general, the drift time and  $m/z$  range decreases with increasing  $n$  for these ions. Signal corresponding to higher charge state families was also observed at higher  $m/z$  (not shown). As previously reported,<sup>45</sup> additional peaks for higher charge states in the  $m/z$  1100 to 1800 region are found in the enantiopure spectrum; these peaks correspond to an elongated rod-like geometry that can only form from the enantiopure solution. The much more intense peak for  $[12\text{Pro}+\text{H}]^+$  in the enantiopure spectrum is ascribed to a closed, icosahedral structure that forms a more favorable hydrogen bonding network than its racemic counterpart.<sup>20</sup>

Integration across the two-dimensional plot yields mass spectra (Figure 1c,d top) that closely resemble those previously

reported for the  $n = 1$  charge state family using IMS-MS.<sup>20,46</sup> Intensities of  $[6\text{Pro}+\text{H}]^+$ ,  $[11\text{Pro}+\text{H}]^+$  and  $[12\text{Pro}+\text{H}]^+$  are noticeably stronger in the spectrum generated using the enantiopure solution. No peaks corresponding to singly charged ions are observed for  $x = 8-10$  or  $x > 12$  from either the racemic or enantiopure solution. Additionally, the intensity of the  $[5\text{Pro}+\text{H}]^+$  cluster ion is noticeably enhanced when electrospraying the racemic sample.

Examination of the  $n = 2$  charge state mass spectra (Figure 1c,d bottom) reveals significant changes as a result of chiral composition. Clusters produced from the racemic solution appear to follow a nearly bimodal distribution that is centered at  $[13\text{Pro}+2\text{H}]^{2+}$  and  $[20\text{Pro}+2\text{H}]^{2+}$  cluster sizes.<sup>46</sup> The distribution of clusters produced from electrospraying the enantiopure solution does not appear to follow either a normal or bimodal distribution. Noticeably, the intensities of the  $[18\text{Pro}+2\text{H}]^{2+}$  and  $[23\text{Pro}+2\text{H}]^{2+}$  ions are enhanced in the enantiopure sample. The  $[14\text{Pro}+2\text{H}]^{2+}$  species is enhanced in the racemic sample. Although a number of ions exhibit varying intensities in the different solutions, several are observed to have significant differences. In summary,  $x = 6, 11,$  and  $12$  ( $n = 1$ ) and  $18$  and  $23$  ( $n = 2$ ) clusters have greater intensity when the enantiopure solution is electrosprayed, and  $x = 5$  ( $n = 1$ ) and  $14, 20, 21, 22$  ( $n = 2$ ) clusters are significantly more intense when produced from the racemic solution.

**Variations with Enantiomeric Composition.** To understand chiral preference in more detail, proline solutions with varying enantiomeric compositions (L:D: 100:0, 80:20, 60:40, 50:50, 40:60, 20:80, 0:100) were electrosprayed. Each solution was run in triplicate for statistical analysis. The intensity obtained for each cluster for  $n = 1$  and  $n = 2$  was ratioed to the total ion signal intensity for the two-dimensional nested spectrum collected using the particular solution. The entire spectrum should not display a chiral preference, and normalizing to it compensates for any variation in electrospray conditions. Results of representative cluster sizes,  $[3\text{Pro}+\text{H}]^+$ ,  $[5\text{Pro}+\text{H}]^+$ ,  $[6\text{Pro}+\text{H}]^+$ ,  $[17\text{Pro}+2\text{H}]^{2+}$ , and  $[18\text{Pro}+2\text{H}]^{2+}$  are shown in Figure 2. A cluster exhibiting no chiral preference will be produced equally effectively from electrospraying all seven solutions, and thus a constant ratio will be observed (e.g.,  $[3\text{Pro}+\text{H}]^+$ ). By contrast, clusters that exhibit a preference for homochirality will be more abundant when sampled from enantiopure solutions, and thus will exhibit a “V-shaped” distribution (e.g.,  $[6\text{Pro}+\text{H}]^+$ ). Clusters that exhibit a preference for heterochirality will be more abundant when sampled from the racemic solution, and thus will exhibit an inverted V “ $\Lambda$ ” distribution (e.g.,  $[5\text{Pro}+\text{H}]^+$ ).<sup>8</sup> These results show that proline molecular clusters exist in three possible states of chiral selectivity: homochiral, heterochiral, and statistical (i.e., having no chiral preference). This type of resolution and “anti-resolution” has been reported previously in our lab for several serine clusters in the  $n = 2$  charge state family.<sup>8</sup> Although the larger proline cluster sizes are not reported here, earlier studies demonstrated that nanometer scale cluster sizes ( $x = \sim 50$  to 100) showed chirally selective elongated structures.<sup>45</sup> These elongated structures exhibited a sharp “V” distribution, where no intensity was observed from the racemic solution.

**Isotopic Analysis.** As a second test of chiral preference, an isotopic labeling technique is used.<sup>3,11</sup> Although isotopic analysis becomes increasingly difficult for larger clusters due to overlapping  $m/z$  features, such features within clusters in the  $n = 1$  charge state family are easily resolved. In these clusters,

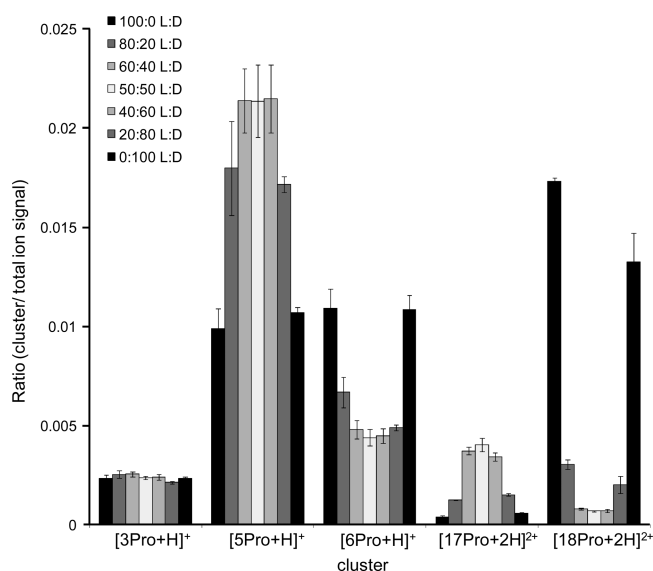


**Figure 2.** Cluster formation ratios obtained upon electro spraying L- and D- proline solutions. The ratios represent relative cluster intensity for solution compositions varying from 100% pure L- to 100% pure D- proline for clusters:  $[3\text{Pro}+\text{H}]^+$ ,  $[5\text{Pro}+\text{H}]^+$ ,  $[6\text{Pro}+\text{H}]^+$ ,  $[17\text{Pro}+2\text{H}]^{2+}$ , and  $[18\text{Pro}+2\text{H}]^{2+}$ . Three data sets have been averaged, and error bars represent one standard deviation. See text for details.

the incorporation of each deuterated proline increases the mass by 7. The relative intensity of each peak within the mass spectrum of a cluster is ratioed to the relative intensity expected from a statistical (binomial) incorporation of the deuterated L- proline. Thus, if incorporation of proline shows no chiral preference, the ratios should all be approximately 1. Isotopically labeled data follow the pattern where flat, “V”, and “A” distributions correspond to statistical, homochiral, and heterochiral preferences, respectively.<sup>3,8,11</sup> The preferences observed with the unlabeled analysis are confirmed for the  $n = 1$  charge state as shown in Figure 3.

In the case of  $[5\text{Pro}+\text{H}]^+$ , both methods of analysis strongly indicate a heterochiral preference; however, a 4:1 composition is shown to be preferred using the labeled analysis, whereas a 3:2 composition is shown to be preferred using the unlabeled analysis. The labeled analysis gives a very specific snapshot of

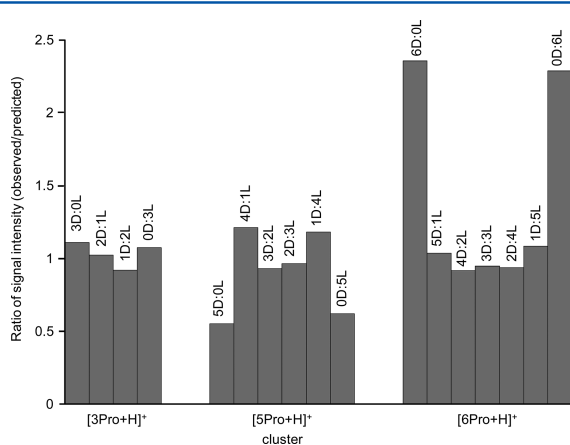


**Figure 3.** Ratio of the observed to predicted (statistical) intensities for the proline clusters:  $[3\text{Pro}+\text{H}]^+$ ,  $[5\text{Pro}+\text{H}]^+$ , and  $[6\text{Pro}+\text{H}]^+$ , where the  $x$  axis refers to the number of L:D prolines in clusters formed from the 50:50 D-proline:L-proline  $[(\text{HN}(\text{CD}_2)_3\text{CD})\text{COOH}]$  mixture.

the actual distribution of the enantiomers in all their permutations in the clusters at the same time, and so, when it can be used (i.e., for the singly charged clusters), the results of the labeled approach are considered more accurate. The error bars for the unlabeled method are also large enough to account for the apparent difference in results.

**Summary of Chiral Preferences.** The results obtained from the unlabeled analysis of clusters in the  $n = 1$  and 2 charge states are summarized in Figure 4. Each point represents the

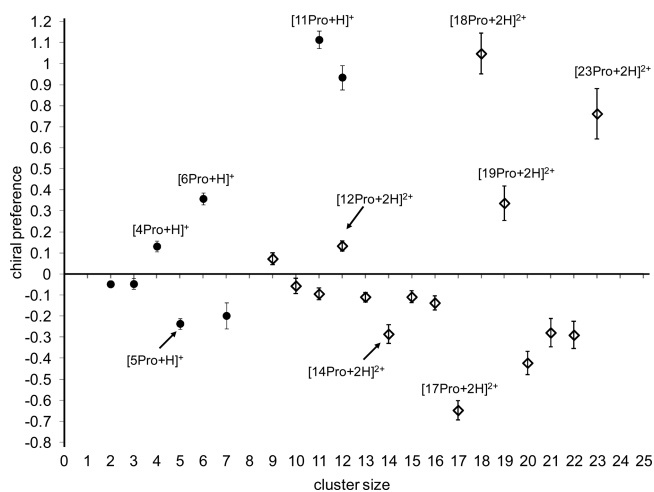


**Figure 4.** Chiral preference plot for  $[x\text{Pro}+n\text{H}]^{n+}$  clusters, where  $x = 2 - 23$  and  $n = 1$  or 2. Positive values indicate a preference for homochirality, and negative values indicate a preference for heterochirality. The chiral preference for each cluster was determined by averaging the difference in intensity for each 100:0, 80:20, 60:40, 50:50, 40:60, 20:80, and 100% L:D data set from the average intensity (see text for details). Error bars represent one standard deviation obtained by collecting each % L:D data set in triplicate.

average deviation of the observed cluster distribution from the predicted distribution for a cluster with no chiral preference, using the following formula to compensate for variation in abundance of clusters:

$$C = \frac{1}{j} \sum_{i=1}^j \frac{|x_i - \bar{x}|}{\bar{x}} \quad (2)$$

where  $C$  is the chiral preference,  $j$  is the number of solutions (7) and  $\bar{x}$  is the average signal intensity (ratioed to the total two-dimensional signal intensity, as described above) of the cluster from all seven solutions. A cluster with no chiral preference would have equal distribution of signal over all seven solutions, corresponding to the flat distribution in Figure 2; the magnitude of its chiral preference in Figure 4 will be zero. As more extreme “V” or “A” distributions in Figure 3 generate larger deviations from the statistical equal distribution, larger magnitudes of chiral preference are recorded. This method for calculating chiral preference is slightly different from a previously reported method,<sup>8</sup> as all seven solutions are used in the calculation, rather than only using a comparison of signals generated from the racemate and the enantiopure solutions. Although absolute chiral preference values differ slightly between the two calculation methods, the trends are the same.

It is worth noting that our results for several clusters in the  $n = 2$  family differ somewhat from those previously reported by Nemes et al.;<sup>9</sup> three of the clusters that they identify as having

strong chiral tendencies ( $[9\text{Pro}+2\text{H}]^{2+}$ ,  $[13\text{Pro}+2\text{H}]^{2+}$ , and  $[15\text{Pro}+2\text{H}]^{2+}$ ) are found to have very little chiral preference in our experiment. The combination of mobility and  $m/z$  separation in our experiment allows multiply charged multimers with the same  $m/z$  ratios to be resolved; with MS alone, as was used by Nemes et al., overlap with signals from larger clusters in higher charge states may complicate measurements of peak intensities.

Based on the chiral preference plot, proline displays a remarkable oscillation in chiral preference values. Notably, the chiral preference of many clusters varies substantially from their nearest neighbor cluster sizes. The smaller  $x = 3$  to 7 ( $n = 1$ ) family shows an odd/even dependence on chiral preference for the 4–7 sizes. Even numbered clusters are homochiral preferring, whereas odd clusters are heterochiral. More pronounced preferences are observed as clusters grow in size. For example,  $[17\text{Pro}+2\text{H}]^{2+}$  shows a strong heterochiral preference, with a value of  $-0.67$ ; with the addition of a single proline monomer,  $[18\text{Pro}+2\text{H}]^{2+}$  exhibits a strong homochiral preference (1.05). This finding is evidence that the formation of these clusters cannot be through the simple build-up of monomers onto an existing core structure; it would be impossible to have such extreme changes in chiral preference for the addition of a single monomer in this manner. Rather, these structures must represent a unique formation event or the combination of smaller nonmonomeric clusters.

If clusters are formed in solution, one might expect that clusters containing the same number of prolines, but carrying different amount of charge, would have the same chiral preference. This is obviously not true for the  $[11\text{Pro}+\text{H}]^+$  (strongly homochirally preferring) and  $[11\text{Pro}+2\text{H}]^{2+}$  (slightly heterochirally preferring) clusters. However, this is not sufficient evidence to show that these clusters do not originate in solution. The strongly homochiral cluster,  $[11\text{Pro}+\text{H}]^+$ , could assemble from either all L- or all D- isomers in a unique formation event or from the combination of clusters with homochiral preference, for example, the combination of 1 (achiral), 4 (homochirally preferring), and 6 (homochirally preferring) proline subunits. By contrast, the  $[11\text{Pro}+2\text{H}]^{2+}$  cluster could form from mixed L- and D- clusters composed of 5 proline (heterochirally preferring) and 6 proline (homochirally preferring) subunits. Both of these types of clusters could originate in solution to form different structures that are protonated differently during the electrospray process. However, it is also possible that one or both of the clusters could assemble in the droplet during the electrospray process.

**Examination of the Origin of Heterochirality in  $[22\text{Pro}+2\text{H}]^{2+}$ .** It is interesting to consider some structures in more detail. While many sizes could be examined for this type of discussion, we focus here on  $[22\text{Pro}+2\text{H}]^{2+}$  which has an experimentally measured cross section of  $410 \pm 5 \text{ \AA}^2$ . One issue that emerges is how D- and L- enantiomers are distributed within a heterochiral cluster. If D- and L- enantiomers were homogeneously distributed, then we would expect no chiral preference. Thus, the locations of the different enantiomers must be key to the structure of the cluster.

One interesting possibility is that D- and L- enantiomers in  $[22\text{Pro}+2\text{H}]^{2+}$  are segregated into domains. An extreme case would be domains made up of 11 L- and 11 D- prolines. Figure 5 shows a hypothetical structure of  $[22\text{Pro}+2\text{H}]^{2+}$ . We propose the formation of the heterochiral  $[22\text{Pro}+2\text{H}]^{2+}$  cluster from two homochiral subunits. This structure is intriguing for us because it can be generated using atomic coordinates for the

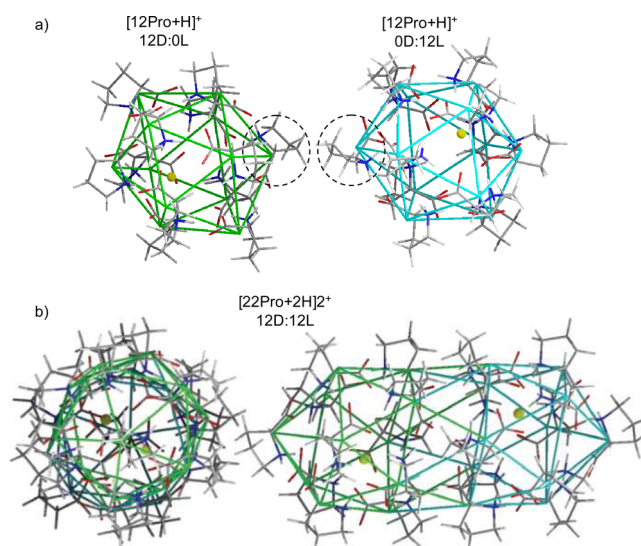


**Figure 5.** Hypothetical structure for heterochiral preferring  $[22\text{Pro}+2\text{H}]^{2+}$ . Note that the D- and L- 11Pro domains lead to a preresolved state.

icosahedral  $[\text{L}-12\text{Pro}+\text{H}]^+$  cluster obtained from previous molecular dynamic simulations.<sup>20</sup> By reflecting atomic coordinates about an arbitrary origin, it is relatively straightforward to obtain an icosahedral  $[\text{D}-12\text{Pro}+\text{H}]^+$  cluster. The  $[\text{D}-12\text{Pro}+\text{H}]^+$  and  $[\text{L}-12\text{Pro}+\text{H}]^+$  structures are fused together by eliminating one proline residue at the end of each cluster and then rotating one structure ( $30^\circ$ ) with respect to the other to optimize hydrogen bonding. Energy minimization of the resulting structure using the InsightII software package (Accelrys, Inc. San Diego, CA) results in a closed geometry. Calculations of theoretical collision cross sections using the trajectory method yield values of  $411 \pm 5 \text{ \AA}^2$ , in good agreement with experiment.<sup>40,41</sup>

The resulting  $[22\text{Pro}+2\text{H}]^{2+}$  cluster is interesting for several reasons. First, like the stable  $[12\text{Pro}+\text{H}]^+$ , which is homochirally preferring,  $[22\text{Pro}+2\text{H}]^{2+}$  forms a closed system that maximizes H-bonding interactions. The segregated L:D composition of this cluster minimizes defects that arise because of mismatches in chirality (as was discussed in the case of heterochiral  $[12\text{Pro}+\text{H}]^+$  geometries). In the case of  $[22\text{Pro}+2\text{H}]^{2+}$ , efficient H-bonded interactions between domains are established by the angular offset between the D- and L- domains (in this case  $[\text{L}-11\text{Pro}+2\text{H}]^{2+}$  and  $[\text{D}-11\text{Pro}+2\text{H}]^{2+}$ ). These stable domains lead to an overall heterochiral species that can be thought of as a preresolved state. That is, addition of another proline monomer of either chirality could result in the elimination of the stable homochiral  $[12\text{Pro}+\text{H}]^+$  having an icosahedral geometry. We note that Cooks and co-workers<sup>47</sup> have reported resolution of homochiral subunits upon dissociation of a heterochiral metal-containing ( $\text{K}^+$ ,  $\text{Rb}^+$ , or  $\text{Cs}^+$ ) serine octamer.

Similar speculations can be used to rationalize the origin of chirality in other cluster sizes. For example, in contrast to  $[22\text{Pro}+2\text{H}]^{2+}$  clusters,  $[23\text{Pro}+2\text{H}]^{2+}$  clusters have a strong homochiral preference. One possible explanation for this is that intermolecular interactions are the most favorable when the  $[23\text{Pro}+2\text{H}]^{2+}$  cluster is formed from  $[\text{L}-11\text{Pro}+2\text{H}]^{2+}$  and  $[\text{L}-12\text{Pro}+2\text{H}]^{2+}$  subunits or  $[\text{D}-11\text{Pro}+2\text{H}]^{2+}$  and  $[\text{D}-12\text{Pro}+2\text{H}]^{2+}$  subunits, but not from mixed L- and D- domains.

Clearly, detailed theoretical investigations of this fascinating behavior would be of interest.

## CONCLUSIONS

The propensity of specific proline clusters to form homo or heterochiral complexes has been investigated with IMS-MS techniques. Remarkably, the chiral makeup of the different clusters oscillates with size. In some cases, a clear trend is established over a cluster size range. In other examples, dramatic shifts in chiral preference are observed with the addition of single monomer subunits. These data suggest that cluster formation does not proceed via the accretion of monomer subunits onto a single core type of structure. Rather, separate species that can be described as stable, simple structures are formed. Additionally, it is proposed that some heterochiral preferring species could be comprised of homochiral subunits of equivalent size.

## AUTHOR INFORMATION

### Corresponding Author

\*E-mail: clemmer@indiana.edu.

### Author Contributions

Both Alison E. Holliday and Natalya Atlasevich contributed equally to this work.

### Notes

The authors declare no competing financial interest.

## ACKNOWLEDGMENTS

The authors wish to acknowledge and funding from the Indiana University METACyt initiative funded from the Lilly Endowment.

## REFERENCES

- (1) Jacques, J.; Collet, A.; Wilen, S. H. *Enantiomers, Racemates, and Resolutions*, John Wiley & Sons: New York, 1981. (reprint ed. 1991, reissued with corrections, Krieger Publishing Company, Malabar, FL, 1994).
- (2) Cooks, R. G.; Zhang, D.; Koch, K. J.; Gozzo, F. C.; Eberlin, M. N. *Anal. Chem.* **2001**, *73*, 3646–3655.
- (3) Julian, R. R.; Hodyss, R.; Kinnear, B.; Jarrold, M. F.; Beauchamp, J. L. *J. Phys. Chem. B* **2002**, *106*, 1219–1228.
- (4) Counterman, A. E.; Clemmer, D. E. *J. Phys. Chem. B* **2001**, *105*, 8092–8096.
- (5) Koch, K. J.; Gozzo, F. C.; Zhang, D.; Eberlin, M. N.; Cooks, R. G. *Chem. Commun.* **2001**, 1854–1855.
- (6) Takáts, Z.; Nanita, S. C.; Cooks, R. G. *Angew. Chem., Int. Ed.* **2003**, *42*, 3521–3523.
- (7) Concina, B.; Hvelplund, P.; Nielsen, A. B.; Nielsen, S. B.; Liu, B.; Tomita, S. *J. Am. Soc. Mass Spectrom.* **2006**, *17*, 275–279.
- (8) Julian, R. R.; Myung, S.; Clemmer, D. E. *J. Am. Chem. Soc.* **2004**, *126*, 4110–4111.
- (9) Nemes, P.; Schlosser, G.; Vékey, K. J. *J. Mass Spectrom.* **2005**, *40*, 43–49.
- (10) Mazurek, U.; Engeser, M.; Lifshitz, C. *Int. J. Mass Spectrom.* **2006**, *249*, 473–476.
- (11) Hodyss, R.; Julian, R. R.; Beauchamp, J. L. *Chirality* **2001**, *13*, 703–706.
- (12) Nanita, S. C.; Takáts, Z.; Cooks, R. G.; Myung, S.; Clemmer, D. E. *J. Am. Soc. Mass Spectrom.* **2004**, *15*, 1360–1365.
- (13) Myung, S.; Julian, R. R.; Nanita, S. C.; Cooks, R. G.; Clemmer, D. E. *J. Phys. Chem. B* **2004**, *108*, 6105–6111.
- (14) Takáts, Z.; Cooks, R. G. *Chem. Commun.* **2004**, 444–445.
- (15) Yang, P.; Xu, R.; Nanita, S. C.; Cooks, R. G. *J. Am. Chem. Soc.* **2006**, *128*, 17074–17086.
- (16) Perry, R. H.; Wu, C.; Neffiu, M.; Cooks, R. G. *Chem. Commun.* **2007**, 1071–1073.
- (17) Spencer, E. A. C.; Ly, T.; Julian, R. R. *Int. J. Mass Spectrom.* **2008**, *270*, 166–172.
- (18) Schalley, C. A.; Weis, P. *Int. J. Mass Spectrom.* **2002**, *221*, 9–19.
- (19) Kong, X.; Lin, C.; Infusini, G.; Oh, H. B.; Jiang, H.; Breuker, K.; Wu, C. C.; Charkin, O. P.; Chang, H. C.; McLafferty, F. W. *ChemPhysChem* **2009**, *10*, 2603–2606.
- (20) Myung, S.; Lorton, K. P.; Merenbloom, S. I.; Fioroni, M.; Koeniger, S. L.; Julian, R. R.; Baik, M. H.; Clemmer, D. E. *J. Am. Chem. Soc.* **2006**, *128*, 15988–15989.
- (21) Knight, W. D.; Clemenger, K.; de Heer, W. A.; Saunders, W. A.; Chou, M. Y.; Cohen, M. L. *Phys. Rev. Lett.* **1984**, *52*, 2141–2143.
- (22) Kroto, H. W.; Allaf, A. W.; Balm, S. P. *Chem. Rev.* **1991**, *91*, 1213–1235.
- (23) Kroto, H. W.; Heath, J. R.; O'Brien, S. C.; Curl, R. F.; Smalley, R. E. *Nature* **1985**, *318*, 162–163.
- (24) Nagashima, U.; Shinohara, H.; Nishi, N.; Tanaka, H. *J. Chem. Phys.* **1986**, *84*, 209–214.
- (25) Lee, S.; Freivogel, P.; Schindler, T.; Beauchamp, J. K. *J. Am. Chem. Soc.* **1998**, *120*, 11758–11765.
- (26) Steinbach, P. J.; Brooks, B. R. *Proc. Natl. Acad. Sci. U.S.A.* **1993**, *90*, 9135–9139.
- (27) Steinberg, M. Z.; Breuker, K.; Elber, R.; Germer, R. B. *Phys. Chem. Chem. Phys.* **2007**, *9*, 4690–4697.
- (28) Uetrecht, C.; Versluis, C.; Watts, N. R.; Wingfield, P. T.; Steven, A. C.; Heck, A. J. R. *Angew. Chem., Int. Ed.* **2008**, *47*, 6247–6251.
- (29) Mason, E. A.; McDaniel, E. W. *Transport Properties of Ions in Gases*; Wiley: New York, 1988.
- (30) St. Louis, R. H.; Hill, H. H. *Crit. Rev. Anal. Chem.* **1990**, *21*, 321–355.
- (31) Hoaglund Hyzer, C. S.; Counterman, A. E.; Clemmer, D. E. *Chem. Rev.* **1999**, *99*, 3037–3079.
- (32) Wittmer, D.; Luckenbill, B. K.; Hill, H. H.; Chen, Y. H. *Anal. Chem.* **1994**, *66*, 2348–2355.
- (33) von Helden, G.; Wyttenbach, T.; Bowers, M. T. *Science* **1995**, *267*, 1483–1485.
- (34) Chen, Y. H.; Siems, W. F.; Hill, H. H. *J. Anal. Chim. Acta* **1996**, *334*, 75–84.
- (35) Hoaglund, C. S.; Valentine, S. J.; Sporleder, C. R.; Reilly, J. P.; Clemmer, D. E. *Anal. Chem.* **1998**, *70*, 2236–2242.
- (36) Hoaglund-Hyzer, C. S.; Li, J.; Clemmer, D. E. *Anal. Chem.* **2000**, *72*, 2737–2740.
- (37) Bluhm, B. K.; Gillig, K. J.; Russell, D. H. *Rev. Sci. Instrum.* **2000**, *71*, 4078–4086.
- (38) Tang, K.; Shvartsburg, A. A.; Lee, H. N.; Prior, D. C.; Buschbach, M. A.; Li, F. M.; Tolmachev, A. V.; Anderson, G. A.; Smith, R. D. *Anal. Chem.* **2005**, *77*, 3330–3339.
- (39) Revercomb, H. E.; Mason, E. A. *Anal. Chem.* **1975**, *47*, 970–983.
- (40) Shvartsburg, A. A.; Jarrold, M. F. *Chem. Phys. Lett.* **1996**, *261*, 86–91.
- (41) Mesleh, M. F.; Hunter, J. M.; Shvartsburg, A. A.; Schatz, G. C.; Jarrold, M. F. *J. Phys. Chem.* **1996**, *100*, 16082–16086.
- (42) Wyttenbach, T.; von Helden, G.; Batka, J. J.; Carlat, D.; Bowers, M. T. *J. Am. Soc. Mass Spectrom.* **1997**, *8*, 275–282.
- (43) Merenbloom, S. I.; Koeniger, S. L.; Valentine, S. J.; Plasencia, M. D.; Clemmer, D. E. *Anal. Chem.* **2006**, *78*, 2802–2809.
- (44) Koeniger, S. L.; Merenbloom, S. I.; Valentine, S. J.; Jarrold, M. F.; Udseth, H.; Smith, R. D.; Clemmer, D. E. *Anal. Chem.* **2006**, *78*, 4161–4174.
- (45) Myung, S.; Fioroni, M.; Julian, R. R.; Koeniger, S. L.; Baik, M. H.; Clemmer, D. E. *J. Am. Chem. Soc.* **2006**, *128*, 10833–10839.
- (46) Julian, R. R.; Myung, S.; Clemmer, D. E. *J. Phys. Chem. B* **2005**, *109*, 440–444.
- (47) Nanita, S. C.; Sokol, E.; Cooks, R. G. *J. Am. Soc. Mass Spectrom.* **2007**, *18*, 856–868.